Article

pubs.acs.org/Biomac

Synthesis of Amylose–Polystyrene Inclusion Complexes by a Facile Preparation Route

Kamlesh Kumar, Albert J. J. Woortman, and Katja Loos*

Department of Polymer Chemistry, Zernike Institute for Advanced Materials, University of Groningen, Nijenborgh 4, 9747 AG, Groningen, The Netherlands

ABSTRACT: The formation of amylose–polystyrene inclusion complexes via a novel two-step approach is described. In the first-step, styrene was inserted inside the amylose helical cavity, followed by free radical polymerization in the second step. The inclusion complexes were characterized by attenuated total reflection fourier transform infrared spectroscopy (ATR-FTIR), ultraviolet spectroscopy (UV), X-ray diffraction (XRD), atomic force microscopy (AFM), and differential scanning calorimetry (DSC). The formation of polystyrene was confirmed by gel permeation chromatography (GPC). The molecular weight of polystyrene can be varied by using amylose bearing different molar masses. The approach described here is general and could be used to synthesize other host–polymer inclusion complexes for which long chains of polymeric guests are difficult to insert into the host cavity.

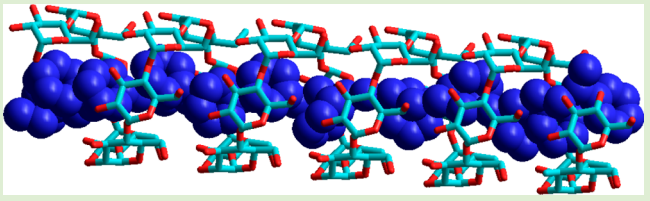

INTRODUCTION

Amylose is a natural linear polysaccharide having α-(1→4) glycosidic linkages.[1] This component constitutes only around 20–30% of starch, compared to 70–80% amylopectin.[2] Amylose can be present in a disordered amorphous phase or helical forms.[3] The helical form can be either a double helix or a single helix, which is also known as a V-amylose. In V-amylose, the hydrophobic cavity (inside the helix of amylose) provides a space for small guest molecules resulting in the formation of inclusion complexes.[3−6] Hydrophobic and van der Waals interactions are the main driving forces for the formation of inclusion complexes between amylose and guest molecules.[7,8] Amylose-inclusion complexes can be used in areas such as molecular imprinting,[9] nanosized delivery systems for unsaturated fatty acids,[10] structuring modeling for starch,[11] and flavor encapsulation in food science.[12]

Until now, two kinds of methods were introduced to synthesize amylose-inclusion complexes. The first method is based on insertion, where hydrophobic guest molecules are inserted inside the amylose helical cavities by direct mixing.[13−15] Some pretreatments can be applied to enhance the amylose–guest interactions.[14−18] In the second approach, known as "vine-twinning polymerization", amylose is synthesized around the guest molecule via enzymatic polymerization.[19−22] Amylose is synthesized from maltoheptaose primers using phosphorylase enzyme, and details are described elsewhere.[23−26]

The vine-twinning polymerization approach was invented to form amylose–polymer inclusion complexes, as the weak hydrophobic interactions are not sufficient to insert long polymer chains in the amylose cavities.[27] However, vine-twinning polymerization is not possible for strongly hydrophobic polymers due to their aggregation in a aqueous buffer solvent.[27] In order to obtain inclusion complexes from strongly hydrophobic polymers, a parallel enzymatic polymerization system was previously performed.[28] However, this parallel system is applicable only to those polymers that can be easily polymerized by enzymes. Moreover, enzymatic polymerization is time-consuming and expensive for mass-scale production compared to the chemical synthesis method.

In this paper we demonstrate a novel, inexpensive, and simple approach to synthesize amylose–polymer inclusion complexes. The approach contains two steps: the monomer is inserted inside the amylose cavity in the first step, followed by polymerization in the second step. The formation of amylose–polystyrene (amylose-PS) inclusion complexes by a two-step procedure is reported. Styrene is in the initial step inserted into amylose, and free radical polymerization of the styrene inside amylose is performed in the second step in order to obtain amylose–PS inclusion complexes. Previously, Kollisch et al. demonstrated living radical polymerizations of CD-complexed styrene in water via the reversible addition–fragmentation chain transfer process.[29] To the best of our knowledge, this is the first study of amylose inclusion complex formation in which a monomer is polymerized inside the helical cavity of amylose to obtain inclusion complexes.

EXPERIMENTAL SECTION

Materials. Amylose with a molecular weight of ~180 kg/mol was purchased from Avebe. Low molecular weight amylose (~43 kg/mol) was prepared by alkali degradation of higher molecular weight amylose.[30] Mica sheets were obtained from Emsdiasum. 2,2′-Azobisisobutyronitrile (AIBN), styrene, and methanol were purchased

Received: March 6, 2013
Revised: April 29, 2013
Published: April 30, 2013

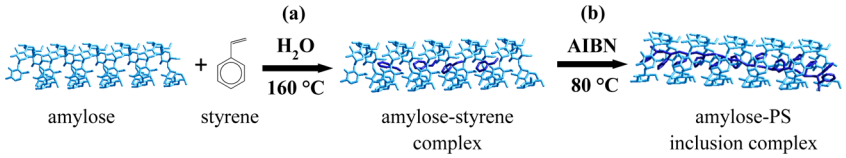

Figure 1. Schematic illustration of the formation of amylose-PS inclusion complexes: (a) inclusion of styrene inside the amylose helical cavity; (b) free radical polymerization of styrene using AIBN.

from Sigma-Aldrich. Styrene was purified by vacuum distillation[31] before use, and other reagents were used as received.

Formation of Inclusion Complexes. *Amylose–Styrene Inclusion Complexes.* Amylose–styrene complexes were prepared by mixing of 1 g of amylose with styrene [5, 10 and 20% (w/w)] in water (15 mL) in screw cap vials and rotated at 85 °C for 4 h to suspend the amylose and styrene in water. Subsequently, the suspension was transferred to a pressure vessel and heated under continuous stirring until the solution temperature reached 160 °C. Afterward, the solution was cooled from 160 to 80 °C in a ventilation oven and rotated overnight to form the complex.

Free Radical Polymerization of Styrene Using AIBN. The amylose–styrene complexes prepared above were mixed with 5% (w/w) AIBN to start the free radical polymerization. The solution was rotated overnight to complete the polymerization of styrene at the same temperature. The final product was precipitated in methanol, and the precipitate was washed with hot water three times before being freeze-dried overnight for further characterization. The yields of product were around 30–35%, which was determined from gravimetric analysis based on the total weight of amylose and styrene.

Removal of PS from Amylose–PS Inclusion Complex. PS was removed from the complex for molecular weight analysis by overnight immersion in toluene.[32] PS solubilized in toluene while amylose still remained as a precipitate. This solution was centrifuged for 20 min at 2000 rpm to reach better separation of precipitated amylose and supernatant PS solution. PS was precipitated in methanol, filtered, and finally dried in a vacuum oven.

Characterization. A Bruker IFS88 FT-IR spectrometer equipped with a MCT-A detector was used to collect infrared spectra, at a resolution of 4 cm^{-1} with an average of 50 scans. UV spectra were recorded on a PYE Unicam SP8–200 spectrophotometer. X-ray diffraction (XRD) measurements were performed on a powder diffractometer (Bruker D8) using CuKα with a wavelength of 1.54 Å as a radiation source. Atomic force microscopy (AFM) images of the samples were obtained in the tapping mode of the Digital Instruments EnviroScope AFM, operated with a Nanoscope IIIa controller using commercial Veeco RTESPW silicon cantilevers (f_o = 240–296 kHz and k = 20–80 N/m as specified by the manufacturer). The samples for AFM were prepared by drop casting of methanol solution (2 mg/mL) on freshly cleaved mica. Differential scanning calorimetry (DSC) scans of the samples were carried out in stainless steel large volume cups against an empty reference cup by Perkin-Elmer Pyris 1 DSC at a heating rate of 10 °C/min from 20 to 160 °C. The samples for DSC were prepared as a suspension of 10% (w/w) in water. GPC measurements were performed in tetrahydrofuran (THF) on a Viscotek GPC operated with model 302 TDA detectors, using 2 columns (Pl-gel 5 μ 30 cm mixed-C from Polymer Laboratories) with a flow rate of 1 mL/min.

RESULTS AND DISCUSSION

Helical amylose has a hydrophobic cavity that enables the inclusion of hydrophobic guest molecules to form amylose-inclusion complexes. As mentioned earlier, it is difficult to form inclusion complexes with very hydrophobic polymers such as PS due to the aggregative nature of PS in aqueous solution. An alternative two-step process was developed as represented in Figure 1 to prepare amylose–PS inclusion complexes. In the first step, styrene was inserted inside the amylose helical cavity, and styrene was then polymerized in the second step to form amylose–PS inclusion complexes. Styrene is a hydrophobic monomer, but it has a relatively lower hydrophobicity compared to PS.[33] Therefore, water can be used as a medium to achieve the inclusion complex. Due to the hydrophobic–hydrophobic interactions, amylose–styrene complexes are formed. Two different molecular weight amyloses were used to synthesize inclusion complexes.

The formation of amylose-PS complexes was confirmed by attenuated total reflection fourier transform infrared spectroscopy (ATR-FTIR) analysis by taking spectra of the initial and final products.[34] Figure 2 shows the spectra of amylose (high

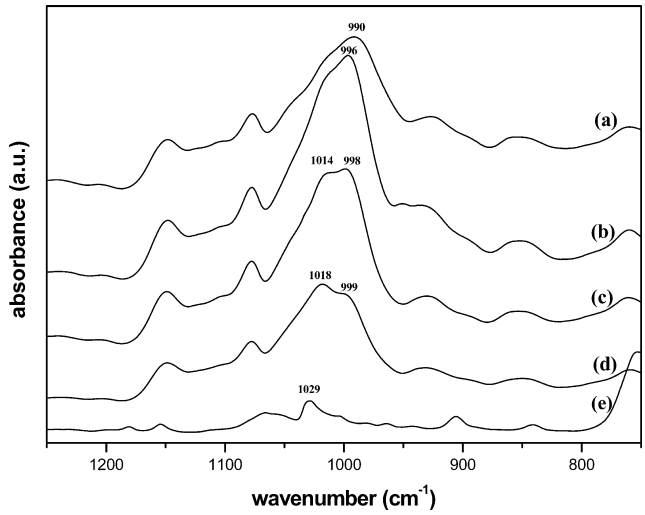

Figure 2. ATR-FTIR spectra of (a) amylose, (b) amylose–PS-5, (c) amylose–PS-10, (d) amylose–PS-20, and (e) PS.

M_w), PS, and amylose–PS inclusion complexes in the region of 700–1250 cm^{-1}. Inclusion complexes of amylose with 5, 10, and 20% (w/w) PS are shown as amylose–PS-5, amylose–PS-10, and amylose–PS-20, respectively. It is clear from the spectra of the inclusion complex that the complex exhibited all absorption bands that are characteristic for amylose. In Table 1 the IR results are summarized. It becomes obvious that the C–O bending vibration (amylose peak) was moved to a higher value in the complexes compared to pristine amylose.

Table 1. Comparison of FTIR Bands of Amylose and Amylose–PS Inclusion Complexes

sample	PS % (w/w)	amylose peak (cm^{-1})	inclusion-complex peak (cm^{-1})
amylose	0	990	no peak
amylose–PS-5	5	996	1012
amylose–PS-10	10	998	1014
amylose–PS-20	20	999	1018

dx.doi.org/10.1021/bm400340k | *Biomacromolecules* 2013, 14, 1955–1960

Furthermore, an additional peak (inclusion-complex peak) appeared in the complexes at around 1012 cm^{-1}. These effects clearly prove the inclusion of PS into the amylose helices.[34]

Furthermore, it becomes obvious that the position of the amylose peak increases to higher wave numbers with increasing % (w/w) of PS. This is due to the higher number of polymer chains inside the helical cavity of amylose. Moreover, with increasing concentration of PS, the intensity of the amylose peak significantly decreased, and the inclusion-complex peak increased.[35]

The synthesis of amylose−PS inclusion complexes was further confirmed by UV spectroscopy.[36,37] The UV absorption spectra of the samples were recorded in a dimethyl sulfoxide (DMSO) solution. PS becomes soluble in DMSO at elevated temperatures,[38] therefore samples were heated at 120 °C for 4h to prepare samples for UV measurements. Figure 3 shows the

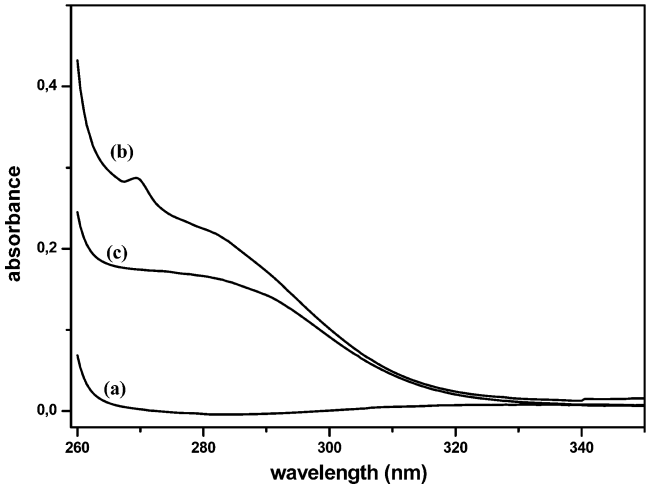

Figure 3. UV spectra of (a) amylose, (b) PS, and (c) amylose−PS-5 complex in DMSO (0.5 mg/mL).

UV spectra of amylose, PS, and amylose−PS-5 complex. As can be seen from Figure 3, the maximum absorbance of PS at 270 nm was absent in the spectrum of the inclusion complex. The complex shows a broad absorbance peak at 288 nm ,which was not present in the spectra of amylose. The appearance of an additional peak in the complex compared to amylose may be due to the stabilized amylose helix due to complexation.

Furthermore, XRD was used to confirm the formation of inclusion complexes. Figure 4 shows the XRD patterns of PS, amylose, and amylose−PS-5 inclusion complex. Amylose shows its typical 2θ peaks at around 17° and 22.7°, and the diffraction peak of PS appeared at 22.5°. The inclusion complex presents two peaks at 13° and 20°, which are the characteristics peaks for the helical inclusion complex structures as described for other amylose−guest inclusion complexes prepared by different approaches.[39,40]

The morphology of the amylose and amylose-PS complexes was evaluated by AFM in the tapping mode. Figure 5 shows amylose (a,b) and amylose-PS-5 (c,d) images in which a and c are the phase images and b and d are the height images, respectively. Changes in the morphology of amylose and amylose-PS-5 due to complex formation can clearly be observed. The homogeneous dispersed amylose chains and the aggregative nature of amylose−PS inclusion complexes becomes clear from the AFM images. This kind of behavior of

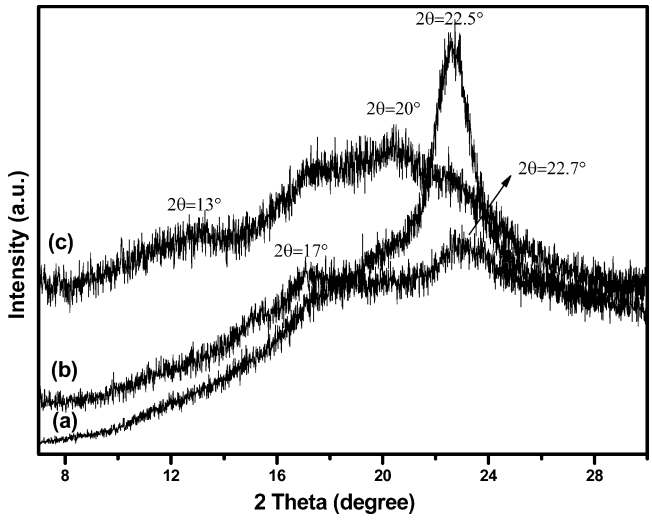

Figure 4. X-ray diffractions of (a) PS, (b) amylose, and (c) amylose−PS-5 inclusion complex.

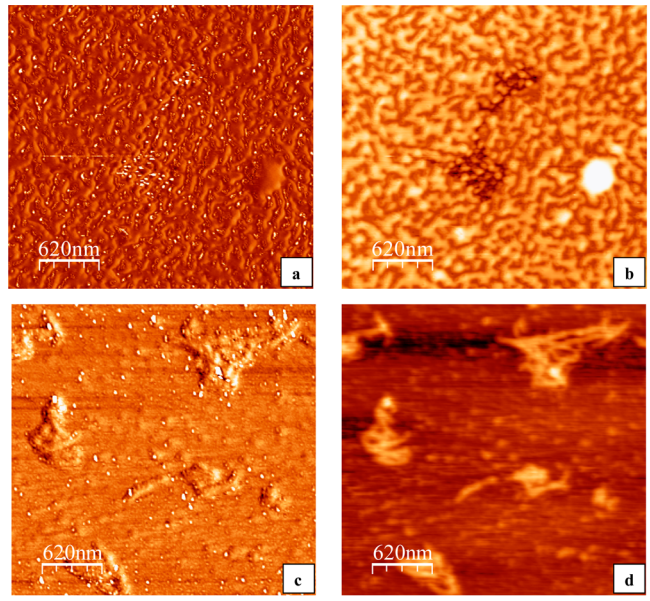

Figure 5. AFM images of amylose exhibit well-disperseed polymer chains ((a) phase, (b) height image), while the amylose−PS-5 complex shows complex aggregates ((c) phase, (d) height image).

amylose inclusion complexes coincides with previous studies of amylose-long chain fatty acid complexes.[12,41]

The thermal behavior of the amylose-PS-5 inclusion complexes in comparison to pristine amylose and PS was studied by DSC (Figure 6). The thermogram obtained from PS showed a characteristic T_g around 100 °C. Compared to amylose and PS, the amylose−PS complex showed a single endotherm at around 117 °C, which was absent in the pristine amylose. This endotherm is due to the dissociation of the inclusion complexes as reported in our previous studies.[11,14] Furthermore, the T_g of PS is not visible in the amylose−PS complex, which indicates that PS is present only as the guest molecules in the amylose helix.

PS chains can be removed from the amylose−PS inclusion complex by washing the complex with toluene.[32] Figure 7 shows spectra of amylose, the unwashed amylose−PS-20 complex, and samples that were washed for 1 min and

dx.doi.org/10.1021/bm400340k | Biomacromolecules 2013, 14, 1955−1960

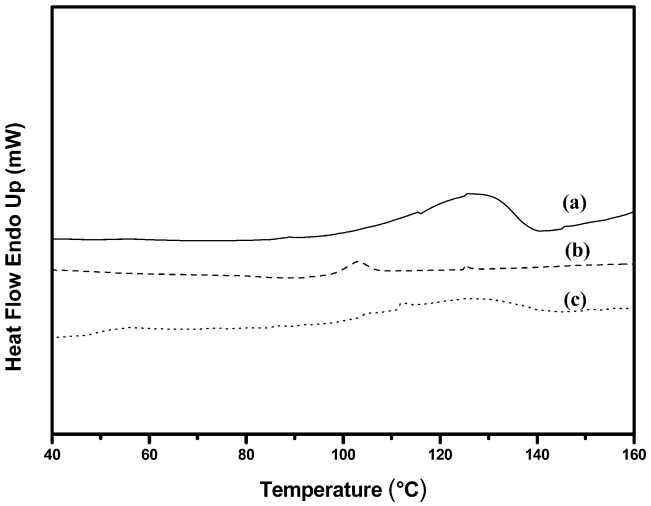

Figure 6. DSC thermograms of (a) amylose–PS-5, (b) PS, and (c) amylose.

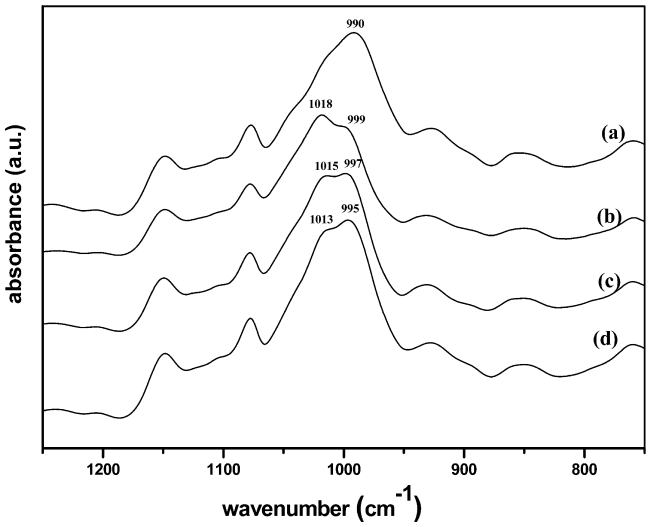

Figure 7. ATR-FTIR spectra of (a) amylose, (b) unwashed amylose–PS-20 complex, (c) sample washed 1 min by toluene, and (d) sample washed by toluene overnight.

overnight, respectively. The intensity of the complex peak was decreased with washing time, while the intensity of the amylose peak increased. It is clear from the spectra that the duration of washing effects the removal of PS. The characteristic peak of the C–O bending vibration of amylose was observed at 995 cm^{-1} after overnight washing, but still did not reach the position of the original amylose peak at 990 cm^{-1}. This shows that some PS remains in the complex even after overnight washing.

GPC was used to determine the molecular weight of PS prepared inside the helical cavity of amylose via free radical polymerization of styrene. Two different molecular weight amyloses (180 kg/mol and 43 kg/mol) were used to obtain PS of different molecular weights. PS was removed from the complex by toluene, followed by precipitation in methanol as described in the Experimental Section. Free radical polymerization of styrene (PS) was also performed without amylose to compare polydispersity of products. GPC results are shown in Figure 8 and are summarized in Table 2. As expected, higher molecular weight PS (PS1) was separated from higher

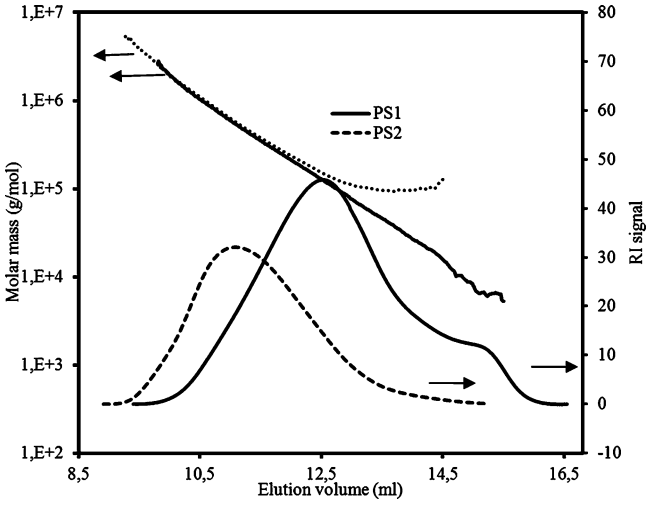

Figure 8. Size exclusion chromatography (SEC) molar mass distributions of PS separated from the amylose–PS inclusion complexes. PS1 was prepared from high molecular weight amylose, and PS2 was prepared from low molecular weight amylose.

Table 2. Molecular Weight of PS prepared in bulk (PS) and PS separated from the amylose–PS Inclusion Complexes Analyzed in THF (PS1 and PS2)

sample	M_w (kg/mol)	Mn (kg/mol)	PDI (M_w/M_n)
PS	722.3	157.7	4.5
PS1	616.5	186.5	3.3
PS2	185.8	45.0	4.1

molecular weight amylose, and lower molecular weight PS (PS2) was obtained from lower molecular weight amylose complexes. The polydispersities obtained are significantly lower than expected for free radical polymerizations (PDI = 4.5), which is in excellent agreement with theoretical studies that have shown this effect for chain growth polymerizations in nanoconfinement (in our case, the inside of the amylose helix).[42–45]

The decreased polydispersity of free radical polymerizations in confinement were observed by other groups as well.[43–46] In the free radical polymerization of styrene/β-cyclodextrin complexes in water[29,47] a decreased polydispersity compared to free radical polymerization was observed as well; however, the effect is stronger in the amylose due to the stronger confinement effect of amylose as compared to cyclodextrin (which can clearly be seen by the fact that increasing molecular weight of amylose decreases the polydispersity of the synthesized PS; see Table 2).

CONCLUSIONS

We have demonstrated a simple two-step method for the synthesis of amylose–PS inclusion complexes. Styrene is introduced inside the hydrophobic helical cavity of amylose in the first step and polymerized via free radical polymerization with AIBN in the second step. The amylose inclusion complexes were characterized in detail by IR spectroscopy and XRD, and their aggregative nature was revealed by AFM. PS can be removed from the complex by washing with toluene for further characterization. Different molecular weight PS was obtained from complexes with amylose of different degrees of polymerization bearing a decreased polydispersity as compared to standard free radical polymerization. This two-step approach

could be used to synthesize various other amylose−polymer inclusion complexes that are difficult to synthesize from other conventional approaches.

AUTHOR INFORMATION

Corresponding Author

*E-mail: k.u.loos@rug.nl.

Notes

The authors declare no competing financial interest.

ACKNOWLEDGMENTS

We thank Joop Vorenkamp for his help in GPC measurements. We are grateful to the group of Solid State Materials for Electronics (Zernike Institute for Advanced Materials, University of Groningen, The Netherlands) for access to the X-ray diffraction spectrometer. This work was financially supported by a VIDI grant from The Netherlands Organization for Scientific Research (NWO).

REFERENCES

(1) Pérez, S., Baldwin, P. M.; Gallant, D. J. Structural Features of Starch Granules. In *Starch: Chemistry and Technology*, 3rd ed.; BeMiller, J., Whistler, R., Eds.; Food Science and Technology, International Series; Academic Press/Elsevier: New York, 2009; Chapter 5, pp 149−192.

(2) Hoover, R. Composition, molecular structure, and physicochemical properties of tuber and root starches: A review. *Carbohydr. Polym.* **2001**, *45*, 253−267.

(3) Wu, H. C.; Sarko, A. The double-helical molecular structure of crystalline α-amylose. *Carbohydr. Res.* **1978**, *61*, 27−40.

(4) Gessler, K.; Uson, I.; Takaha, T.; Krauss, N.; Smith, S. M.; Okada, S.; Sheldrick, G. M.; Saenger, W. V-Amylose at atomic resolution: X-ray structure of a cycloamylose with 26 glucose residues (cyclomaltohexaicosaose). *Proc. Natl. Acad. Sci. U.S.A.* **1999**, *96*, 4246−4251.

(5) Shimada, J.; Kaneko, H.; Takada, T.; Kitamura, S.; Kajiwara, K. Conformation of amylose in aqueous solution: Small-angle X-ray scattering measurements and simulations. *J. Phys. Chem. B* **2000**, *104*, 2136−2147.

(6) Kim, O. K.; Choi, L. S.; Zhang, H. Y.; He, X. H.; Shih, Y. H. Second-harmonic generation by spontaneous self-poling of supramolecular thin films of an amylose−dye inclusion complex. *J. Am. Chem. Soc.* **1996**, *118*, 12220−12221.

(7) Yajima, H.; Nishimura, T.; Ishii, T.; Handa, T. Effect of concentration of iodide on the bound species of I_2/I^-_3 in the amylose−iodine complex. *Carbohydr. Res.* **1987**, *163*, 155167.

(8) Nimza, O.; Gesslera, K.; Usónb, I.; Sheldrickb, G. M.; Saenger, W. Inclusion complexes of V-amylose with undecanoic acid and dodecanol at atomic resolution: X-ray structures with cycloamylose containing 26 D-glucoses (cyclohexaicosaose) as host. *Carbohydr. Res.* **2004**, *339*, 1427−1437.

(9) Kanekiyo, Y.; Naganawa, R.; Tao, H. pH-responsive molecularly imprinted polymers. *Angew. Chem., Int. Ed.* **2003**, *42*, 3014−3016.

(10) Wulff, G.; Avgenaki, G.; Guzmann, M. S. P. Molecular encapsulation of flavours as helical inclusion complexes of amylose. *J. Cereal Sci.* **2005**, *41*, 239−249.

(11) Ahmadi-Abhari, S.; Woortman, A. J. J.; Hamer, R. J.; Oudhuis, A. A. C. M.; Loos, K. Influence of lysophosphatidylcholine on the gelation of diluted wheat starch suspensions. *Carbohydr. Polym.* **2013**, *93*, 224−231.

(12) Zabar, S.; Lesmes, U.; Katz, I.; Shimoni, E.; Bianco-Peled, H. Structural characterization of amylose-long chain fatty acid complexes produced via the acidification method. *Food Hydrocolloids* **2010**, *24*, 347−357.

(13) Kida, T.; Minabe, T.; Okabe, S.; Akashi, M. Partially-methylated amyloses as effective hosts for inclusion complex formation with polymeric guests. *Chem. Commun.* **2007**, 1559−1561.

(14) Rachmawati, R.; Woortman, A. J. J.; Loos, K. A facile preparation method for inclusion complexes between amylose and polytetrahydrofurans. *Biomacromolecules.* **2013**, *14*, 575−583.

(15) Rachmawati, R.; Woortman, A. J. J.; Loos, K. Tunable properties of inclusion complexes between amylose and polytetrahydrofuran. *Macromol. Biosci.* **2013**, DOI: 10.1002/mabi.201300022.

(16) Star, A.; Steuerman, D. W.; Heath, J. R.; Stoddart, J. F. Starched carbon nanotubes. *Angew. Chem., Int. Ed.* **2002**, *41*, 2508−2512.

(17) Shogren, R. L. Complexes of starch with telechelic poly(ε-caprolactone) phosphate. *Carbohydr. Polym.* **1993**, *22*, 93−98.

(18) Fanta, G. F.; Swanson, C. L.; Doane, W. M. Composites of starch and poly(ethylene-*co*-acrylic acid). Complexing between polymeric components. *J. Appl. Polym. Sci.* **1990**, *40*, 811−821.

(19) Kadokawa, J.; Kaneko, Y.; Tagaya, H.; Chiba, K. Synthesis of an amylose−polymer inclusion complex by enzymatic polymerization of glucose 1-phosphate catalyzed by phosphorylase enzyme in the presence of polyTHF: A new method for synthesis of polymer−polymer inclusion complexes. *Chem. Commun.* **2001**, 449−450.

(20) Kadokawa, J.; Kaneko, Y.; Nakaya, A.; Tagaya, H. Formation of an amylose−polyester inclusion complex by means of phosphorylase-catalyzed enzymatic polymerization of α-D-glucose 1-phosphate monomer in the presence of poly(ε-caprolactone). *Macromolecules* **2001**, *34*, 6536−6538.

(21) Kaneko, Y.; Kadokawa, J. Synthesis of nanostructured bio-related materials by hybridization of synthetic polymers with polysaccharides or saccharide residues. *J. Biomater. Sci., Polym. Ed.* **2006**, *17*, 1269−1284.

(22) Kaneko, Y.; Kadokawa, J. Vine-twining polymerization: A new preparation method for well-defined supramolecules composed of amylose and synthetic polymers. *Chem. Rec.* **2005**, *5*, 36−46.

(23) Vlist, J. v. d.; Reixach, M. P.; Maarel, M. v. d.; Dijkhuizen, L.; Schouten, A. J.; Loos, K. Synthesis of branched polyglucans by the tandem action of potato phosphorylase and *Deinococcus geothermalis* glycogen branching enzyme. *Macromol. Rapid Commun.* **2008**, *29*, 1293−1297.

(24) Ciric, J.; Loos, K. Synthesis of branched polysaccharides with tunable degree of branching. *Carbohydr. Polym.* **2013**, *93*, 31−37.

(25) Vlist, J. v. d.; Schonen, I.; Loos, K. Utilization of glycosyltransferases for the synthesis of a densely packed hyperbranched polysaccharide brush coating as artificial glycocalyx. *Biomacromolecules* **2011**, *12*, 3728−3732.

(26) Ciric, J.; Oostland, J.; De Vries, J. W.; Woortman, A. J.; Loos, K. Size exclusion chromatography with multi detection in combination with matrix-assisted laser desorption ionization-time-of-flight mass spectrometry as a tool for unraveling the mechanism of the enzymatic polymerization of polysaccharides. *Anal. Chem.* **2012**, *84*, 10463−10470.

(27) Kadokawa, J. Preparation and applications of amylose supramolecules by means of phosphorylase-catalyzed enzymatic polymerization. *Polymers* **2012**, *4*, 116−133.

(28) Kaneko, Y.; Saito, Y.; Nakaya, A.; Kadokawa, J.; Tagaya, H. Preparation of inclusion complexes composed of amylose and strongly hydrophobic polyesters in parallel enzymatic polymerization system. *Macromolecules* **2008**, *41*, 5665−5670.

(29) Kollisch, H.; Barner-Kowollik, C.; Ritter, H. Living free radical polymerization of cyclodextrin host−guest complexes of styrene via the reversible addition fragmentation chain transfer (RAFT) process in aqueous solution. *Macromol. Rapid Commun.* **2006**, *27*, 848−853.

(30) Lai, Y.-Z.; Sarkanen, K. V. Kinetic study on the alkaline degradation of amylose. *J. Polym. Sci., Part C: Polym. Symp.* **1969**, *28*, 15−26.

(31) Schmaus, P.; Mezder, W. G. Procedure for the distillation of vinylaromatic monomers in the presence of oxygen and 4-tertiary-butylcatechol as polymerization inhibitors, U.S. Patent 2002/0040845, 2002.

(32) Howell, B. A.; Cui, Y.; Priddy, D. B. Assessment of the thermal degradation characteristics of isomeric poly(styrene)s using TG, TG/MS and TG/GC/MS. *Thermochim. Acta* **2003**, *396*, 167−177.

(33) Mcgovern, J. J.; Grim, J. M.; Teach, W. C. Determination of monomer in polystyrene: Spectrophotometric and solubility methods. *Anal. Chem.* **1948**, *20*, 312−314.
(34) Maciejewska, W.; Polewski, K.; Wyspianska, M. G. A spectroscopic study of amylose−Rose Bengal complexes. *Carbohydr. Res.* **1991**, *226*, 179−183.
(35) Sambasevam, K. P.; Mohamad, S.; Sarih, N. M.; Ismail, N. A. Synthesis and characterization of the inclusion complex of β-cyclodextrin and azomethine. *Int. J. Mol. Sci.* **2013**, *14*, 3671−3682.
(36) Rodríguez, S. D.; Bernik, D. L.; Mereau, R.; Castet, F.; Champagne, B.; Botek, E. Amylose−vanillin complexation assessed by a joint experimental and theoretical analysis. *J. Phys. Chem. C* **2011**, *115*, 23315−23322.
(37) Wulff, G.; Steinert, A.; Holler, O. Modification of amylose and investigation of its inclusion behavior. *Carbohydr. Res.* **1998**, *307*, 19−31.
(38) Subramaniam, A. B.; Lecuyer, S.; Ramamurthi, K. S.; Losick, R.; Stone, H. A. Particle/fluid interface replication as a means of producing topographically patterned polydimethylsiloxane surfaces for deposition of lipid bilayers. *Adv. Mater.* **2010**, *22*, 2142−2147.
(39) Kadokawa, J.; Kaneko, Y.; Nagase, S.; Takahashi, T.; Tagaya, H. Vine-twining polymerization: Amylose twines around polyethers to form amylose−polyether inclusion complexes. *Chem.—Eur. J.* **2002**, *8*, 3321−3326.
(40) Seneviratne, H. D.; Biliaderis, C. G. Action of α-amylases on amylose−lipid complex superstructures. *J. Cereal. Sci.* **1991**, *13*, 129−143.
(41) Lesmes, U.; Cohen, S. H.; Shener, Y.; Shimoni, E. Effects of long chain fatty acid unsaturation on the structure and controlled, release properties of amylose complexes. *Food Hydrocolloids* **2009**, *23*, 667−675.
(42) Tribet, C.; Provata, A.; Nicolis, G. Lattice model for polymer propagation in confined media. *J. Chem. Phys.* **1994**, *100*, 6082−6087.
(43) Begum, F.; Simon, S. L. Modeling methyl methacrylate free radical polymerization in nanoporous confinement. *Polymer* **2011**, *52*, 1539−1545.
(44) Malvaldi, M.; Bruzzone, S.; Picchioni, F. Confinement effect in diffusion-controlled stepwise polymerization by Monte Carlo simulation. *J. Phys. Chem. B* **2006**, *110*, 12281−12288.
(45) Iwasaki, T.; Yoshida, J. I. Free radical polymerization in microreactors. Significant improvement in molecular weight distribution control. *Macromolecules* **2005**, *38*, 1159−1163.
(46) Uemura, T.; Ono, Y.; Kitagawa, K.; Kitagawa, S. Radical polymerization of vinyl monomers in porous coordination polymers: Nanochannel size effects on reactivity, molecular weight, and stereostructure. *Macromolecules* **2008**, *41*, 87−94.
(47) Uyar, T.; Rusa, M.; Tonelli, A. E. Polymerization of styrene in cyclodextrin channels: Can confined free-radical polymerization yield stereoregular polystyrene? *Macromol. Rapid Commun.* **2004**, *25*, 1382−1386.